Pergamon

0045-7930(94)00017-4

Computers & Fluids Vol. 24, No. 1, pp. 63–79, 1995

0045-7930/95 $9.50 + 0.00

AN EFFICIENT MULTIGRID APPROACH TO SOLVING HIGHLY RECIRCULATING FLOWS

N. G. WRIGHT[1] and P. H. GASKELL[2]

[1]Department of Civil Engineering, University of Nottingham, Nottingham NG7 2RD, U.K.

[2]Department of Mechanical Engineering, University of Leeds, Leeds LS2 9JT, U.K.

(Received 1 June 1993; in revised form 18 April 1994)

Abstract—A multigrid solution strategy is presented for the efficient and economic solution of highly recirculating incompressible laminar flows. This paper emphasizes the importance of using high order discretizations for the governing equations of motion, in particular the inertia terms, and the enhancement of the overall stability and efficiency of the method through the use of defect correction. The latter enables solutions to an accuracy equivalent to machine round-off to be found easily with solutions to 'engineering accuracy' being obtained very rapidly on extremely fine grids. These ideas are demonstrated for the solution of two commonly encountered test problems—flow in a lid-driven cavity and flow through a suddenly expanding channel. Results show that proceeding in this way leads to a robust methodology for the solution of a whole class of problems of this type, which is readily extended to three dimensions.

1. INTRODUCTION

Increased reliance on computers as a means of investigating fluid flows of practical interest is placing ever greater demands on computational fluid dynamicists to provide:

- improved models for important physical phenomena such as turbulence or combustion,
- flexible grid generation and domain decomposition,
- discretization techniques embodying increased accuracy,
- economic solution procedures for large systems of algebraic equations.

From an engineering standpoint all four are of equal importance, however it is the latter two which form the principal theme of this paper—the formulation of a robust, nonlinear, multigrid, high order, bounded, unsegregated solution strategy for confined, highly recirculating, laminar flows.

Although a streamfunction-vorticity formulation of the governing equations has some advantages it is now common practise to use primitive variables to represent the flow in the context of engineering applications. This is usually accompanied by the use of a staggered grid arrangement in order to avoid solutions containing pressure oscillations, an approach which is followed here—work with colocated grids is reported elsewhere [1]. The choice of a suitable and preferably accurate discrete approximation to the nonlinear inertial terms present in the governing equations needs careful consideration. Low order approximations are notorious for introducing numerical (or false) diffusion into solutions whilst high order ones are noted for their inherent lack of boundedness. A recent study [2] has however made it possible for solutions to be obtained with a combined high order bounded convective transport approximation and nonlinear multigrid approach.

The choice of a suitable smoother for the velocity and pressure field is a key component of the overall solution strategy and should not be underestimated, since an inefficient smoother can severely degrade multigrid convergence rates [3].

The well-known SIMPLE technique [4] has been implemented in a multigrid environment [5]. However, it represents a segregated (or decoupled) solver—that is, the velocity and pressure fields are decoupled and solved sequentially, the latter being determined via a derived pressure equation. Another solver which falls into this category is the Distributive Gauss–Seidel (DGS) method, proposed by Brandt [6]. An obvious disadvantage of such an approach is the use of frozen variables in the solution at each stage of the calculation.

Recently attempts [7–9] have been made to devise methods that solve the variables simultaneously, in an unsegregated fashion, thus maintaining the physical coupling between them.

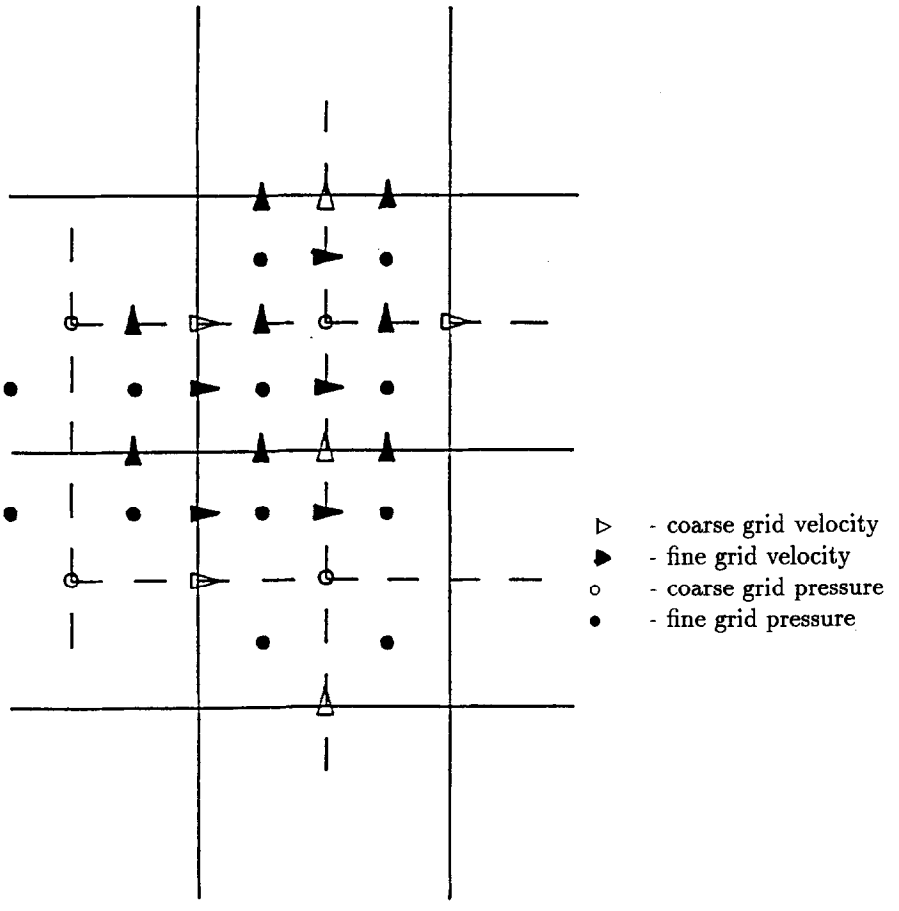

Fig. 1. Staggered grid and coarsening.

References [7] and [8] are more complex than Symmetric Coupled Gauss Seidel (SCGS) [9] or as it is called here, the Block Implicit Method (BIM), which is easily comprehended and efficient. With the BIM each velocity component is incremented twice. The method's simplicity and low operation count make it the ideal choice for use with, and in the development of, a multigrid solution strategy. The method can be applied point-by-point or extended to a line solution technique [10, 11]. Both approaches are investigated here. Unlike SIMPLE, prior to the start of this work the authors were unaware of any theoretical smoothing analysis of the BIM, hence an intuitive approach had to be adopted in performing the computations. It was re-assuring to subsequently discover from an independent source that analysis [12] reveals the latter to have a superior smoothing rate.

The discretization procedure adopted is discussed in Section 2 and is followed by a detailed description of the preferred smoother, both point and line versions. Treatment of boundary conditions is given in Section 3 together with a solution to the well known lid-driven cavity problem [13]. Section 4 introduces the theory of multigrids, before defining a complete multigrid strategy for use with the BIM. The application of this strategy is demonstrated in Section 5 and accompanying results are presented in Section 6 along with the results for the additional test problem of the flow over a suddenly expanding channel. Finally, in Section 7, the merits of this combined overall solution procedure are reviewed.

2. EQUATIONS OF MOTION AND NUMERICAL FORMULATION

2.1. Governing Equations

For steady-state, incompressible laminar flow the non-dimensional governing equations of motion, written in Cartesian tensor form, are:

$$\frac{\partial(u_j u_i)}{\partial x_j} = -\frac{\partial p}{\partial x_i} + \frac{1}{\mathrm{Re}}\frac{\partial^2 u_i}{\partial x_j^2} \tag{1}$$

$$\frac{\partial u_j}{\partial x_j} = 0 \tag{2}$$

where Re is the Reynolds number.

2.2. *Discretization Procedure*

The method used to discretize the inertia terms present in equation (1) is extremely important in the case of convection dominated flows since it can greatly influence the quality of the solution. The characteristic lack of boundedness, associated with a typical high order approximation, in regions of the flow containing steep gradients in one or more of the dependent variables has ensured the continued widespread use of the well known, low order, numerically diffuse hybrid [14] scheme in complex flow situations. This in turn has lead to an element of complacency with regard to the presence of false diffusion in solutions. It is argued that grid refinement can satisfactorily alleviate this problem.

For many flows of a practical nature the above compromise represents a rather simplistic view; for example, experience shows that for flow in a lid-driven cavity at a Reynolds number of 1000 a mesh size as small as 1/500 may be required to obtain a grid independent solution with hybrid differencing. Similarly a 25% error in the solution of the same problem at a Reynolds number of 5000, on a grid containing 128^2 points, is easily demonstrated. Also in a recent paper Gaskell and Lau [2] show that one would need to employ a vastly greater number of grid nodes, $O(10^3)$ with hybrid, than with their new high order scheme, to achieve the same level of accuracy for the solution of a simple (yet demanding) test problem. The same is also found to be true in more complex flow situations [15]. Unfortunately, the use of grids as fine as these are not a practical option in the case of general three-dimensional flows. Storage requirements are a severe restriction, particularly as the number of dependent variables (and thus the number of equations to be solved) increases in proportion to the complexity of the physics involved.

In the present work equations (1) and (2) were written in discrete form using the staggered grid arrangement and control volume formulation—shown in Fig. 1. Applying Gaskell and Lau's high order Curvature Compensated Convective Transport (CCCT) [2] generic approximation to a two-dimensional computational domain then, for a control volume centred at the $(i-1,j)$th node of a uniform grid (with $u_{i-1/2,j} > 0$) gives the value of a scalar, ϕ, at the right hand face, as:

$$\phi_{i-1/2,j} = (\tfrac{3}{4} + 2\alpha)\phi_{i-1,j} + (\tfrac{3}{8} - \alpha)\phi_{i,j} - (\tfrac{1}{8} + \alpha)\phi_{i-2,j} \tag{3}$$

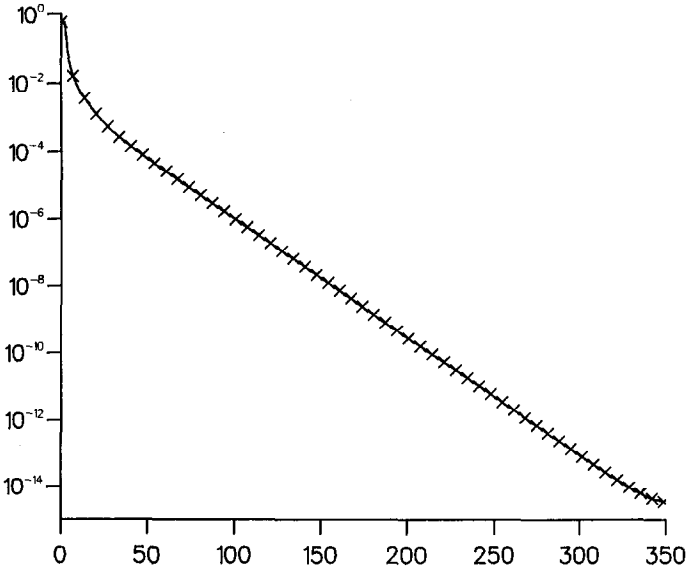

Fig. 2. Log of residual against Fine Grid Work Units for the driven cavity with Re = 1000, $n = 64$, and tolerance = 10^{-10}.

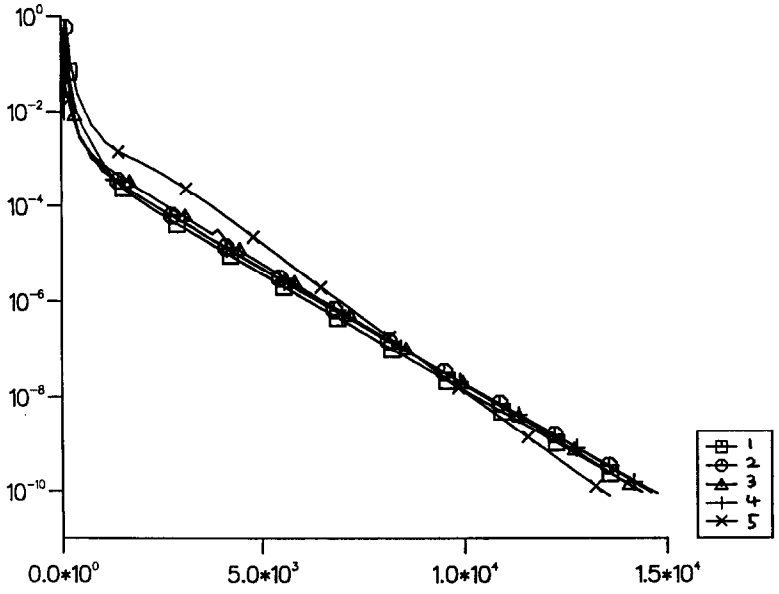

Fig. 3. Log of residual against Fine Grid Work Units for the driven cavity with various forms of defect correction on a grid of 256 × 256 points.

which has a leading truncation error term of $O(\alpha h^2)$, where α is an optimal parameter and h is the size of the grid spacing. Initially, α was set equal to zero, representing maximum accuracy and making equation (3) equivalent to Leonard's [16] QUICK approximation. Later the use of the SMART [2] algorithm for determining α is demonstrated. Other well known approximations to convective transport can be generated by simply selecting an appropriate value for α. Diffusion terms were approximated in the standard way by central differencing. Also, for comparison purposes, results obtained with hybrid differencing of the convective terms are reported.

3. THE BLOCK IMPLICIT METHOD (BIM)

The BIM is relatively straight forward and easily comprehended. Proceeding as if for a two-dimensional calculation, four velocities and one pressure, corresponding to the same control volume, are updated simultaneously by inverting a 5 × 5 matrix. The details of the implementation

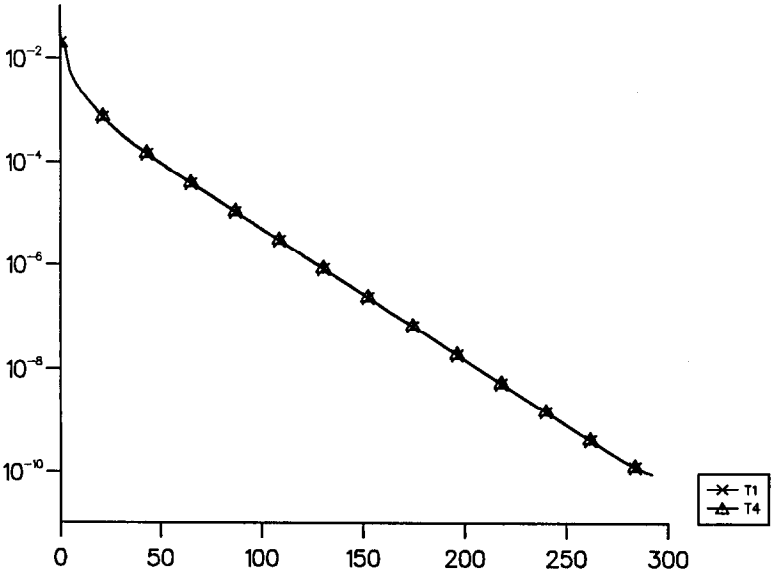

Fig. 4. Log of residual against Fine Grid Work Units for the driven cavity with SMART and QUICK discretization.

adopted here differ in several ways from Vanka's SCGS [9] approach (in terms of the treatment of relaxation, discretization and line solution) and are thus outlined in full below.

3.1. A Point-by-Point Formulation

Consider the control volume shown in Fig. 1. The control volumes are visited in turn with the result that each velocity is updated twice—it has been observed that this ensures the stability lacking with a single update. The difference equations are given by:

$$\sum A^u_{k,l} u_{k,l} + \frac{p_{m+1,n} - p_{m,n}}{h} = 0 \quad \text{for } u_{m,n},\ m = i \text{ and } i-l,\ n = j, \tag{4}$$

$$\sum A^v_{k,l} v_{k,l} + \frac{p_{m,n+1} - p_{m,n}}{h} = 0 \quad \text{for } v_{m,n},\ m = i,\ n = j \text{ and } j-1, \tag{5}$$

and

$$\frac{u_{i,j} - u_{i-1,j}}{h} + \frac{v_{i,j} - v_{i,j-1}}{h} = 0 \tag{6}$$

Writing in terms of residuals (r) and corrections ($'$) and neglecting coefficients of velocities apart from central ones, gives:

$$\begin{bmatrix} A^u_{i,j} & 0 & 0 & 0 & -\frac{1}{h} \\ 0 & A^u_{i-1,j} & 0 & 0 & \frac{1}{h} \\ 0 & 0 & A^v_{i,j} & 0 & -\frac{1}{h} \\ 0 & 0 & 0 & A^v_{i,j-1} & \frac{1}{h} \\ \frac{1}{h} & -\frac{1}{h} & \frac{1}{h} & -\frac{1}{h} & 0 \end{bmatrix} \begin{bmatrix} u'_{i,j} \\ u'_{i-1,j} \\ v'_{i,j} \\ v'_{i,j-1} \\ p'_{i,j} \end{bmatrix} = \begin{bmatrix} r^u_{i,j} \\ r^u_{i-1,j} \\ r^v_{i,j} \\ r^v_{i,j-1} \\ r^c_{i,j} \end{bmatrix} \tag{7}$$

This diagonal, doubly-bordered, sparse matrix can be decomposed into lower and upper diagonal (LU) form, the unknown values being found efficiently by forward and back substitution [17]. As a result of the linearization involved in the calculation of the coefficients A^u and A^v from values at the previous iterate, the corrections need to be under-relaxed. In this work values between 0.5 and 0.7 for velocity and 1.3 and 1.6 for pressure were used. The line solver was more robust and in general the values used were higher. Iteration proceeds until the modulus of the residual given by the $\|\cdot\|_2$ norm defined below is less than a prescribed value, taken after examining results at various tolerances to be 10^{-4}.

$$\|r\|_2 = \left(\frac{\sum_{i,j} (r^{u2}_{i,j} + r^{v2}_{i,j} + r^{c2}_{i,j})}{3 \times n \times n} \right)^{1/2} \tag{8}$$

3.2. A Line by Line Formulation

Some of the relaxation techniques mentioned in Section 1 solve the variables along a line simultaneously (i.e. all variables ϕ_{ij}, $i = 1, \ldots n$, with $j =$ constant or vice versa). This is often thought to be preferable to solving point-by-point, due to better treatment of the coupling between variables in what is a more implicit solution procedure. Furthermore, earlier work [18] indicates that CPU times increase markedly with an increase in Reynolds number when applying the point version of the BIM, and that a line solver may therefore be beneficial. The line formulation implemented here solves on a line of constant j all the variables v_{ij}, p_{ij}, u_{ij-1}, u_{ij} for $i = 1, \ldots, n$ and although it is found to be computationally more expensive than the point solver, its fully

Table 1. CPU times for the BIM solution of the two-dimensional driven cavity on the Silicon Graphics 4D/480

	Re = 100		Re = 1000	
Grid	hybrid	QUICK	hybrid	QUICK
2^2	0.00 s	0.00 s	—	—
4^2	0.02 s	0.04 s	0.15 s	—
8^2	0.52 s	0.45 s	0.84 s	4.67 s
16^2	6.28 s	5.52 s	6.58 s	28.05 s
32^2	1 min 22.94 s	1 min 13.39 s	58.26 s	2 min 33.51 s
64^2	20 min 26.43 s	17 min 36.54 s	11 min 31.68 s	24 min 41.55 s
128^2	5 h 13 min 2.37 s	4 h 4 min 43.17 s	2 h 2 min 41.76 s	5 h 34 min 43.58 s

implicit nature allows for a complete evaluation of the line solver. The consequence being that if such a solver is not superior to the point one, then other less implicity line solvers [3] will probably offer no advantage.

The structure of the solution matrix is exploited to the full, in order to solve it as efficiently as possible. The vector of variables for a line of constant j is:

$$\{v_{1j}, p_{1j}, v_{1j-1}, u_{1j}, v_{2j}, p_{2j}, v_{2j-1}, u_{2j}, \ldots v_{ij}, p_{ij}, v_{ij-1}, u_{ij}, \ldots v_{nj}, p_{nj}, v_{nj-1}, u_{nj}$$

and this is represented as

$$\underline{w} = \{\underline{w_1}, \underline{w_2}, \ldots, \underline{w_i}, \ldots, \underline{w_N}\}$$

where $\underline{w_i} = \{v_{ij}, p_{ij}, v_{ij-1}, u_{ij}\}$. This requires the solution of the matrix equation:

$$A\underline{w} = \underline{r} \tag{9}$$

where A is tridiagonal which can be decomposed into LU form and solved by backward and forward substitution. Obviously, A, L and U are all matrices whose entries are themselves 4×4 matrices which are inverted in the course of the algorithm.

3.3. Sweeping Procedures

When sweeping through the grid it is common practice to visit each control volume in the direction of increasing i then j. However, this is obviously not the only way of proceeding; i or j could decrease or j could change before i. There are, of course, eight different possibilities:

1(5) $i(j)$—increasing followed by $j(i)$—increasing,
2(6) $i(j)$—decreasing followed by $j(i)$—increasing,
3(7) $i(j)$—increasing followed by $j(i)$—decreasing,
4(8) $i(j)$—decreasing followed by $j(i)$—decreasing.

The relative performance of each of these is affected by the predominant flow direction, so to choose any particular one would not be meaningful for the general case. A combination of some sort would be preferable. Several permutations were investigated and the following one selected: 1 followed by 4 then 5 then 8.

For the line-by-line case the solution sweeps through the domain four times in the direction of j increasing, j decreasing, i increasing and i decreasing. In other matters the solution procedure is the same as for the point-by-point solver.

3.4. Boundary Conditions

Two techniques for implementing the boundary conditions for momentum have been employed previously. One uses values positioned on the boundaries and amends the near wall calculation to

Table 2. The different combinations of schemes evaluated for defect correction

case	smoother	residual
1	upwind	hybrid
2	upwind	QUICK
3	hybrid	central
4	hybrid	QUICK
5	QUICK	QUICK

Table 3. Selected data comparing the defect correction solutions on a 256^2 grid at Reynolds number of 1000 to a tolerance of 10^{-10}. The subscripts m denotes the local extremum in the main vortex

Scheme	ψ_m	x	y	ω_m
1	0.102328428561E + 00	0.52340	0.42974	1.769344232581
2	0.115222561641E + 00	0.52340	0.42974	2.022297162212
3	0.113343861574E + 00	0.52340	0.42974	1.986152868512
4	0.115222563512E + 00	0.52340	0.42974	2.022297161544
5	0.115222562452E + 00	0.52340	0.42974	2.022297163112

take account of this. The other uses 'mirror' nodes outside the boundary that are set so as to satisfy the boundary conditions. The first technique is common practice [19] and has been successfully applied to a wide range of complex problems. Leonard [16], on the other hand, is known to favour the second approach but has only reported results for simple test cases. Both techniques were evaluated during the present study. Although the second method is easier to program and requires less CPU time per iteration (there are less logical expressions to evaluate), it was found to require more iterative steps, so it actually used more CPU time than the first technique. Also at high Reynolds numbers it was often unstable, particularly when used in conjunction with a multigrid technique. Therefore when, as is the case here, high order discretization is used for the inertia terms the near-boundary values of velocity perpendicular to the boundary were approximated by switching to hybrid differencing in order to calculate the near-boundary flux.

In the test problems considered in the subsequent sections there is no boundary condition for pressure. This problem is resolved by fixing the value of the pressure (normally zero) at a pre-determined reference point. Then after each iteration the new value of the pressure there is subtracted from the value at all the nodes spanning the solution domain. Other researchers have taken this point to lie at one of the corners. Here, instead, the value at the centre was chosen—the pressure there being calculated as the average of its value at the four surrounding nodes. This procedure is just as efficient as the other but when multigrids are employed ensures easier comparison between pressures on different grid levels.

3.5. Assessment of the BIM

In order to assess the suitability of the BIM as a potential smoother for use with multigrids the problem of the two-dimensional lid-driven cavity was solved for Reynolds numbers of 100 and 1000, with mesh spacings ranging from 1/4 to 1/128.

CPU times for hybrid and QUICK generated on a Silicon Graphics 4D/480 machine are shown in Table 1. It can be seen that for both schemes the CPU time obeys the power-law relationship:

$$\text{CPU} \propto n^{\beta} \tag{10}$$

where $\beta \approx 1.8$ and n is the number of finite difference nodes. It is apparent that solutions on grids with more than 128^2 nodes are impractical with the BIM as it stands. Even if it were possible to achieve convergence, then with QUICK differencing at a Reynolds number of 1000 the time required to obtain a solution on a grid containing 256^2 nodes say, would be in the region of 75 h—an estimate based on the above relationship.

Table 4. Selected data at Reynolds number 1000 for a grid of 1024 × 1024 for comparison of QUICK and SMART the subscripts are the same as in Table 3 with the addition of the secondary left and right corner vortices denoted by r and l and the tertiary left and right corner vortices denoted by rr and ll

Disc.	QUICK	SMART
ψ_m	0.11866	0.11866
x	0.52930	0.52390
y	0.43164	0.43164
ω_m	2.0641	2.06413
ψ_r	−0.23141e − 3	−0.23143e − 3
x	0.08008	0.08008
y	0.91992	0.91992
ω_r	−0.34367	−0.34366
ψ_r	−0.017392e − 2	−0.17330e − 2
x	0.86133	0.86133
y	0.88477	0.88477
ω_l	−1.1335	−1.1333

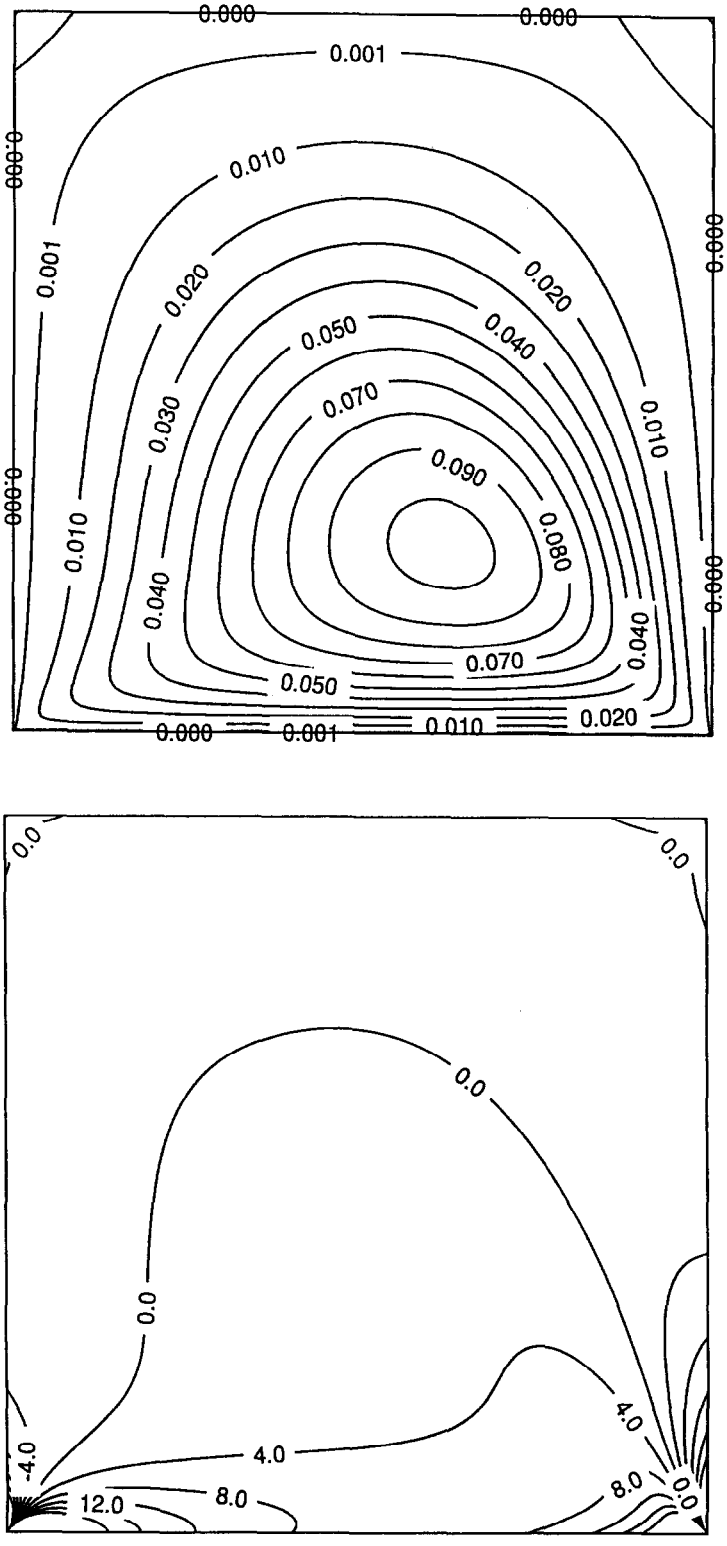

Fig. 5. Streamfunction and vorticity for the driven cavity at Re = 100.

Table 5. CPU seconds and convergence rate θ for BIMM at Reynolds number 100

	hybrid		QUICK		SMART	
Grid	CPU s	Conv. rate θ	CPU s	Conv. rate θ	CPU s	Conv. rate θ
4^2	0.66	0.574	0.89	0.629	0.74	0.663
8^2	1.12	0.538	1.61	0.590	1.37	0.596
16^2	3.06	0.541	4.25	0.552	3.90	0.586
32^2	10.87	0.496	13.93	0.483	12.13	0.501
64^2	38.68	0.420	44.58	0.380	42.33	0.415
128^2	135.45	0.296	150.23	0.291	132.90	0.296
256^2	472.65	0.255	581.93	0.249	503.38	0.255
512^2	1857.20	0.245	2369.20	0.244	2065.15	0.245
1024^2	8842.08	0.277	11509.18	0.275	10188.90	0.275

The results of selected data such as maximum streamfunction for QUICK differencing on a grid of 128×128 compare well with those of Ghia *et al.* [20] in Table 7, who used a coupled strongly-implicit method with a streamfunction-vorticity formulation and multigrid algorithm for h as small as 1/256. Their results are very accurate not only because of the small grid spacing employed, but also as a result of the fact that ψ and ω are calculated directly—not indirectly as in the present work. The indirect calculation can introduce errors due to the approximations involved.

4. MULTIGRID FORMULATION

A current serious constraint on the application of CFD techniques to real problems is that of limited resolution vis-à-vis a restriction on the number of grid nodes that can be employed. From the test problem considered in the previous section it is found that with QUICK a grid of 64^2 nodes is required for accurate solutions, although one of 32^2 gives a qualitatively correct answer that would suffice in some situations. However, the solution to many problems is often found on very coarse grids containing approx. 16^2 nodes. These have proved to be very inaccurate, especially when hybrid differencing is used to approximate convective transport. A hybrid solution to the above lid-driven cavity on a 16^2 grid at a Reynolds number of 1000 results in an error of 46% for the value of the maximum streamfunction relative to that obtained by Ghia *et al.* [20]. Clearly, when solution techniques are extended to encompass three-dimensional flow situations these problems are exacerbated.

Hitherto, the principle research activity aimed at overcoming the above problems has been targeted at designing iterative schemes with higher error reductions. However, these still have the disadvantage of deteriorating convergence rates as the iteration proceeds. The one idea that has opened the door to the practical and accurate solution of such flows is the concept of multigrids, which was outlined briefly in Section 1. The method seeks to obtain the initial fast convergence of an ordinary scheme throughout the iteration procedure, thus giving very fast solutions. Below the theory of multigrids is discussed more fully, various components of the overall approach and those specific to the methodology described here are examined in relation to the two-dimensional lid-driven cavity problem.

4.1. Multigrid Theory

When observing the convergence of a non-multigrid iterative technique it can be seen that initially convergence is rapid, but that this soon stops and error reduction becomes very slow. This

Table 6. CPU seconds and convergence rate θ for BIMM at Reynolds number 1000

	hybrid		QUICK		SMART	
Grid	CPU s	Conv. rate θ	CPU s	Conv. rate θ	CPU s	Conv. rate θ
4^2	0.68	0.624	—	—	—	—
8^2	1.34	0.693	3.62	0.946	—	—
16^2	4.20	0.673	10.39	0.853	—	—
32^2	16.25	0.677	33.22	0.818	32.62	0.869
64^2	68.48	0.684	87.69	0.699	94.32	0.709
128^2	343.97	0.737	263.03	0.622	282.44	0.625
256^2	1153.70	0.636	854.80	0.543	924.01	0.546
512^2	3687.76	0.527	3066.08	0.491	3532.70	0.511
1024^2	14313.05	0.488	12404.90	0.463	13419.76	0.464

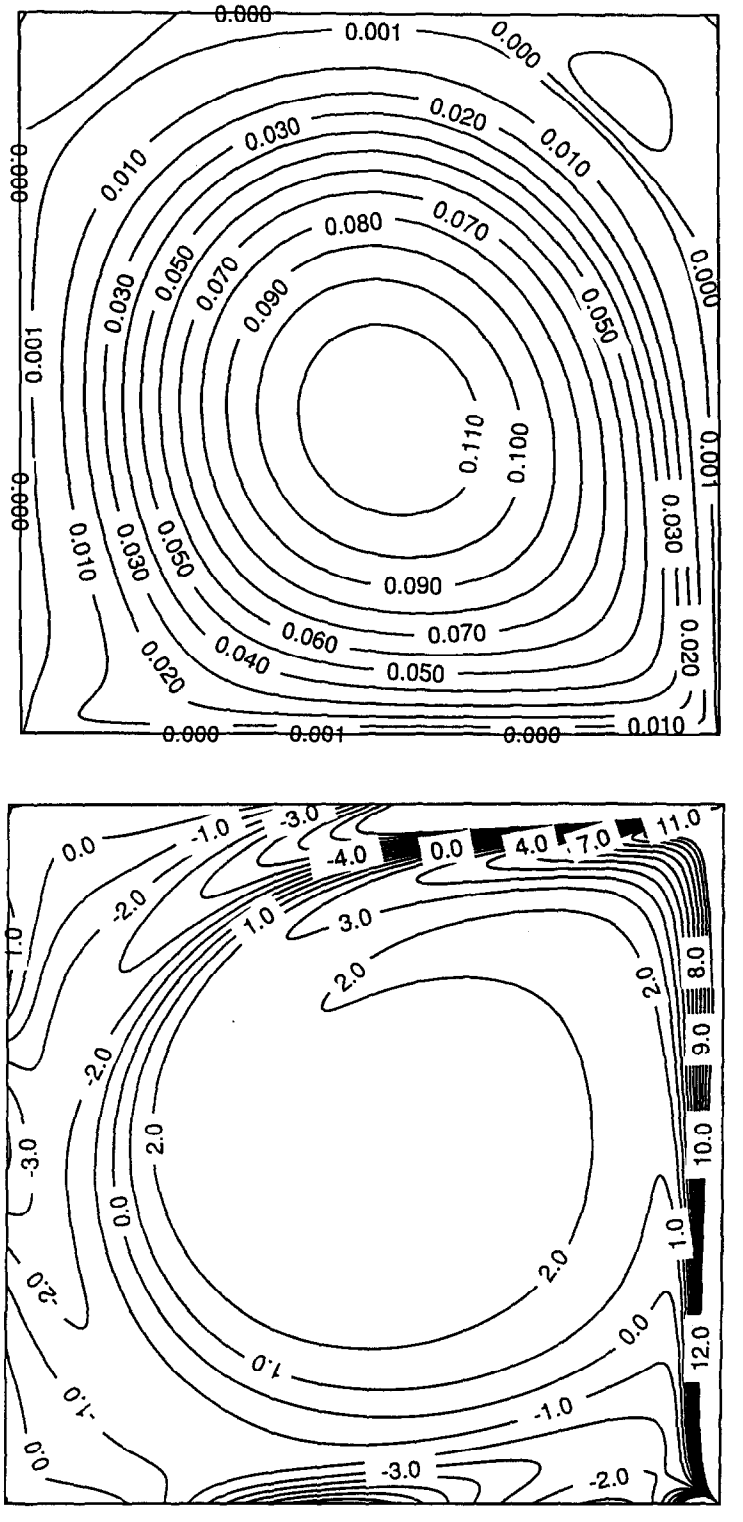

Fig. 6. Streamfunction and vorticity for the driven cavity at Re = 1000.

Table 7. Selected data for BIMM with 1024^2 points

	Re = 100			Re = 1000		
Disc.	hybrid	SMART	GGS	hybrid	SMART	GGS
ψ_m	0.103516	0.103519	0.103423	0.118696	0.118821	0.117927
x	0.6157	0.6157		0.5308	0.5308	0.5313
y	0.2622	0.2622	0.2656	0.4341	0.4341	0.4375
ω_m	3.17044	3.17046	3.16646	2.05888	2.06337	2.04968
ψ_l	−1.79705E − 06	−1.79817E − 06	−1.74877E − 6	−2.33135E − 04	−2.35445E − 04	−2.31129E − 4
x	0.0337	0.0337	0.0313	0.0825	0.0825	0.0859
y	0.9653	0.9653	0.9609	0.9214	0.9214	0.9219
ω_l	−1.46139E − 02	−1.46152E − 02	−1.55509E − 2	−0.35090	−0.35194	−0.36175
ψ_r	−1.27312E − 01	−1.27336E − 05	−1.25374E − 5	−1.72713E − 03	−1.73142E − 03	1.75102E − 3
x	0.9419	0.9419	0.9453	0.8638	0.8638	0.8594
y	0.9380	0.9380	0.9375	0.8872	0.8872	0.8906
ω_r	−3.50668E − 02	−3.50654E − 02	−3.30749E − 2	−1.11374	−1.11118	−1.15465
ψ_{ll}	4.33481E − 06	4.33276E − 06	—	6.08160E − 09	1.46830E − 08	—
x	0.0493	0.0493	—	0.0044	0.0034	—
y	0.9468	0.9468	—	0.9946	0.9927	—
ω_{ll}	−4.30330E − 02	−4.30363E − 02	—	2.72809E − 03	3.81468E − 03	—
ψ_{rr}	3.14914E − 10	3.17386E − 10	—	4.89003E − 08	4.99971E − 08	9.31929E − 8
x	0.9966	0.9966	—	0.9917	0.9917	0.9922
y	0.9956	0.9956	—	0.9917	0.9917	0.9922
ω_{rr}	2.08628E − 04	2.08796E − 04	—	8.93567E − 03	8.86485E − 03	8.52782E − 3

is a manifestation of the efficiency of an iterative solver in eliminating errors of wavelength similar to the mesh size only. In order to maintain this fast convergence and exploit this property of iterative solvers, multigrid methods solve the problem on a hierarchy of coarser grids. This has the added advantage that iterations on coarser grids takes less time. Equations on coarser grids are amended to ensure that they represent the actual solution on the finer grids by the adding of a source term. Here, because the Navier–Stokes equations are non-linear we use the Full Approximation Storage (FAS) version of multigrids.

For full details of the theory readers are referred to an earlier text [18, 21]. It has been shown theoretically by Brandt and Dinar [6] (who first proposed these techniques) that such an algorithm will be very efficient. It should result in grid independent convergence and so require the same number of iterations for any grid level. Having selected an appropriate multigrid approach the next step is to see how this can be combined with the BIM to yield an efficient solution procedure.

4.2. *A Block Implicit Multigrid Method (BIMM)*

Several multigrid strategies have been proposed and implemented for cycling between grids in order to smooth errors efficiently. The one used here differs from those of Shaw and Sivaloganathan [22] and Brandt and Dinar [6]:

(1) The system of equations is constructed on each grid level $k = 1, \ldots, m$.
(2) The solution on the coarsest grid is smoothed using the BIM for a fixed number of iterations.
(3) The difference between the initial and final solution on the current grid level is calculated. This is the correction to the corresponding fine-grid which is prolonged and added to the solution there.
(4) If the new grid is not the finest, m, stages (2) and (3) repeated.
(5) Once the finest grid level has been reached, the solution there is smoothed for a fixed number of iterations.

Table 8. Convergence rate for the line version at Reynolds number 1000

	hybrid	QUICK	SMART
Grid	Conv. rate	Conv. rate	Conv. rate
4^2	0.487	0.797	—
8^2	0.527	0.901	—
16^2	0.557	0.863	—
32^2	0.678	0.818	0.876
64^2	0.744	0.711	0.728
128^2	0.761	0.620	0.623
256^2	0.656	0.539	0.544
512^2	0.522	0.438	0.442
1024^2	0.418	0.366	0.367

Table 9. Reattachment lengths for various Reynolds numbers

Re	Reat. Length
100	1.1090
200	1.7078
400	2.6477

One multigrid iteration consists of executing the above sequence once iterations are continued until the residual on the fine-grid is less than a specified tolerance. The multigrid cycling strategy is based on a fixed V-cycle of [23] which has been successfully implemented for a variety of problems in compressible flows. More sophisticated adaptive cycling strategies such as W- and F-cycle were evaluated, but offered no advantage at the Reynolds numbers of interest.

In the following multigrid calculations, the residual measure and relaxation factors were taken to be the same as those used for the ordinary BIM computations. Note that in the formulation of the BIM given in the previous section, in terms of residuals and updates, is advantageous for use with multigrids, since the values of the residuals are readily available for transfer to coarser grids.

4.3. Restriction and Prolongation

The grid coarsening procedure adopted is illustrated in Fig. 1. A grid reduction factor of 2 is used. One coarse grid scalar cell coincides with four fine-grid scalar cells. The velocity cells for each grid are orientated in line with what one would expect with a procedure for a one-grid technique; this means that coarse and fine-grid velocity cells do not coincide.

The nature of the restriction and prolongation operators is dictated by the grid arrangement. Linear interpolation is used for the restriction of velocities, and bi-linear interpolation for the restriction of scalars. The boundaries are not restricted since they are fixed. Prolongation is similarly carried out using linear and bi-linear interpolation.

There is one aspect of coarsening and interpolation that deserves special mention. Consider the source term that is added to the coarse grid equations,

$$I_k^{k-1}r^k + L^{k-1}(I_k^{k-1}q^k), \tag{11}$$

along with a point (i_c, j_c) on the coarse-grid and the four associated fine-grid points (i_f, j_f), (i_f+1, j_f), (i_f, j_f+1) and (i_f+1, j_f+1), where $i_f = 2i_c - 1$ and $j_f = 2j_c - 1$. By examining the residual of the continuity equation, on the coarse grid level, for the interpolated velocities and the interpolation of the fine-grid residual of continuity in terms of the fine-grid velocities, it can be shown that they are the same, so that:

$$I_k^{k-1}r^k + L^{k-1}(I_k^{k-1}q^k) = 0 \tag{12}$$

Thus the coarse-grid RHS for the continuity equation is zero. When implementing the algorithm this RHS could be computed along with that for the other equations. However, this is seen to be unnecessary from the above analysis. In fact it would be disadvantageous to do so, as this would give values to machine round-off error rather than zero. Sivaloganathan and Shaw [22] have also discussed this feature. They refer to it as "*continuity satisfaction*", that is, if continuity is satisfied on the fine grid it is automatically satisfied on the coarse-grid. They also state that this method of coarsening gives rise naturally to compatible momentum control volumes, but this is not the case since momentum control volumes on different grids do not coincide. Oosterlee and Wesseling

Table 10. Fine grid work units and convergence rate θ for the sudden expansion in a pipe using SMART discretization and 256 by 4096 mesh points

	100		200		400	
Grid	FGWU	Conv. rate θ	FGWU	Conv. rate θ	FGWU	Conv. rate θ
2^2	92.00	0.922	58.00	0.878	—	—
4^2	58.75	0.821	59.25	0.862	—	—
8^2	42.06	0.766	67.56	0.874	—	—
16^2	24.44	0.570	32.52	0.629	—	—
32^2	18.16	0.486	23.54	0.608	38.87	0.793
64^2	14.89	0.420	21.24	0.592	28.41	0.664
128^2	14.06	0.386	15.65	0.405	20.77	0.556
256^2	13.85	0.385	12.58	0.337	20.53	0.570

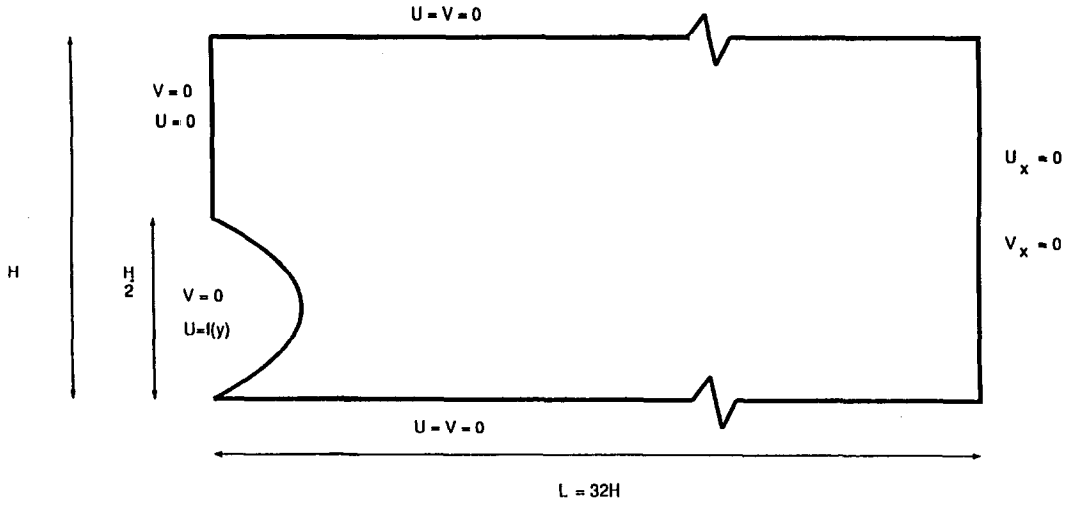

Fig. 7. The geometry and boundary conditions for the sudden expansion.

[24] use a volume average to interpolate momentum residuals. This was assessed, but found to offer no appreciable advantages.

5. APPLICATION OF THE BIMM

The above BIMM was applied to the test problem described in Section 3, namely the two-dimensional lid-driven cavity. Once again, solutions were obtained for Reynolds numbers of 100 and 1000 with both hybrid and QUICK discretization. The maximum number of internal nodes employed was 1024^2. A Full Multigrid (FMG) algorithm was used, that is, a solution on a coarse-grid was obtained and prolonged to form an initial solution on the next fine-grid level. On the coarsest grid initial conditions of zero were used, that is, $\underline{\mathbf{u}} = p = 0$ for all $\underline{\mathbf{r}} = 0$.

With respect to the pressure condition Brandt and Dinar [6] advise that this should only be applied on one grid level. It was found, however, that applying it on all grid levels had no effect on the convergence rate. It was sufficient, though, to only apply it on the coarse-grid. This strategy was adopted to save CPU time. Sivaloganathan and Shaw have also observed this phenomenon.

Figure 2 shows the log of residual against FGWU for a grid of 64×64 points to a tolerance of 10^{-10}. This is a straight line which shows that optimal multigrid convergence has been achieved. The fine-grid work unit is a measure of the total work done on all grids expressed in terms of the work required for one fine-grid iteration.

5.1. Defect Correction

Before considering full solutions and CPU times, the concept of "*defect correction*" is examined. This concept derives from examining the problem of choosing between a low order stable and efficient discretization such as hybrid and a high order less stable and computationally more expensive one such as QUICK to approximate convective transport. When smoothing in multigrid algorithm, all that is required is to smooth the error on the current grid, not eliminate it. So the accuracy of the discretization is not relevant. The only criteria are stability and efficiency. So it would appear natural to use a low order discretization for smoothing and implement a high order discretization through a correction to the source term in the equation. This is the basis of the defect correction method as outlined by Hackbusch [25]. To find a new iteration u^{n+1} from the equation,

$$L\underline{u}^{n+1} = \underline{r}^n \tag{13}$$

requires the use of two operators

- L^l—lower order discretization for smoothing
- L^h—high order discretization for residual calculation.

The following system needs to be solved,

$$L^l\underline{u}^{n+1} = \underline{r}^n + L^l\underline{u}^n - L^h\underline{u}^n \tag{14}$$

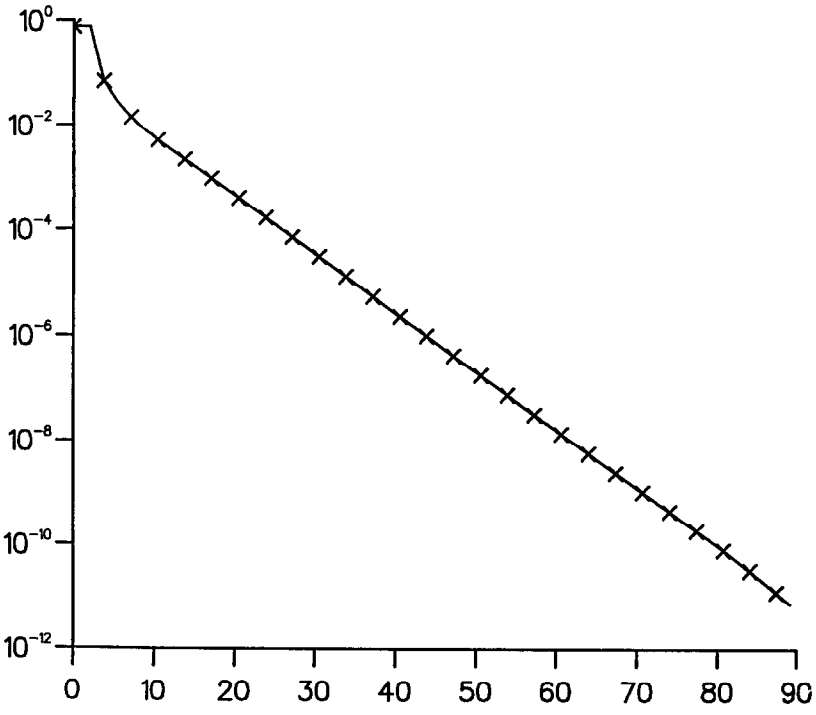

Fig. 8. Log of residual against Fine Grid Work Units for the sudden expansion for Re = 100, 200 and 400.

This has been implemented in five cases as shown in Table 2. Obviously case 5 is not defect corrected, but is included for comparison.

From Fig. 3 it can be seen that all five converge very quickly initially and the four defect correction cases reach solutions of engineering accuracy ($\approx 10^{-3}$) faster than QUICK/QUICK. It should also be noted that in these cases all the methods, with the exception, of QUICK/QUICK, were able to start from zero initial conditions. QUICK/QUICK required an initial condition from another grid to prevent divergence. This instability is also reflected in the slower initial convergence. Only when the residual is down to 10^{-8} does QUICK/QUICK perform better. The worse convergence for cases 1–4 is caused by the delayed implementation of the QUICK terms, i.e. once every multigrid iteration. Table 3 gives values of maximum streamfunction (ψ_m), position (x, y) and vorticity (ω_m) at this point. Those obtained with the same discretizations for residual calculation are identical to eight decimal places, demonstrating that the choice of discretization scheme for smoothing has no effect on the eventual solution.

In view of its superior stability and convergence it was decided to proceed only with defect correction. Upwind/QUICK was adopted for maximum stability and efficiency in smoothing and accuracy in solution.

5.2. Implementation of the SMART algorithm

As mentioned earlier initial implementation of CCCT was performed with $\alpha = 0$. This is identical to Leondard's QUICK scheme which can be prone to unphysical under and/or overshoots. These are problematic for turbulent calculations and may affect accuracy in this laminar case. So for the multigrid program to be fully applicable and amenable to extension to more complex physical phenomena and geometries, Gaskell and Lau's [2] SMART algorithm for determining α was implemented. For details of the latter, readers are referred to their work. Having developed the defect correction as part of the multigrid strategy it is very easy and computationally efficient to implement SMART, with the feature of α values only being calculated within the defect correction in the source term. From Fig. 4 it can be seen that convergence histories for SMART and QUICK are practically identical. Furthermore the results for maximum streamfunction and such data are very close, with SMART just a little more accurate than QUICK—see Table 4. The present implementation of SMART differs from that of Gaskell and Lau in two ways. Firstly, α is not

stored at each point and so is not under-relaxed. Secondly, the algorithm has been adapted to prevent divide by zero problems that maybe encountered when calculating normalized face values.

6. RESULTS

At a glance the results reveal that the times required with multigrid are significantly lower than those found with the ordinary BIM [see Tables 1, 5 and 6—the bracketed numbers are predictions based on the power law relation, equation (10)]. It is not certain however, that given the necessary CPU time a solution could be obtained in the standard way on the finest grids quoted—there is evidence [20] that the use of so fine a grid makes ordinary schemes unstable. The only reason that multigrid solutions were not obtained on even finer grids was the limit on the core memory space available on the Silicon Graphics machine.

With reference to Tables 5 and 6 one can compare the relative performance of hybrid, QUICK and SMART when used as the high order scheme in the defect correction. On coarse grids SMART and QUICK have higher convergence rates than hybrid. On finer grids though the opposite occurs. It was not possible to obtain full solutions at Reynolds number 1000 with a finest grid level of less than 32^2 with SMART, but coarse grids of 2^2 were used as the coarsest in the multigrid algorithm to obtain corrections. An examination of Table 7 shows that there are differences in the value of key variables between hybrid and SMART particularly in the tertiary vortices at Reynolds number of 1000 due to higher gradients. These are only slight, due to the extremely fine grids used. Results for these fine grids are shown as contours in Figs 5 and 6.

The convergence rate, θ, which is shown in Tables 5 and 6 is defined as:

$$\theta = \left[\frac{\text{final residual}}{\text{initial residual}}\right]^{1/\text{FGWU}} \tag{15}$$

As one might expect, from the above results, the rates obtained with the BIMM are much lower than those that would be obtained with non-multigrid BIM. The multigrid convergence rates decrease (on the whole) as mesh size decreases, and optimality is achieved. This, along with the plots of log of residual against FGWU confirms that optimal multigrid behaviour has been obtained. Optimal behaviour is achieved at coarser grid levels for lower Reynolds numbers, because the governing equations are 'less' non-linear.

It can be seen that there is little difference between the convergence rates obtained with the three discretizations on the different grid levels, at Reynolds number 100. The sudden drop in the convergence rate experienced with hybrid between the two grid levels, 128^2 and 256^2 was also observed by Linden *et al.* [27]. This is caused by a change to the predominant use of central differencing within the solution domain as the cell Reynolds number falls below 2. Upwind differencing, with its inherent grid-dependent numerical diffusion, limits convergence rate [28].

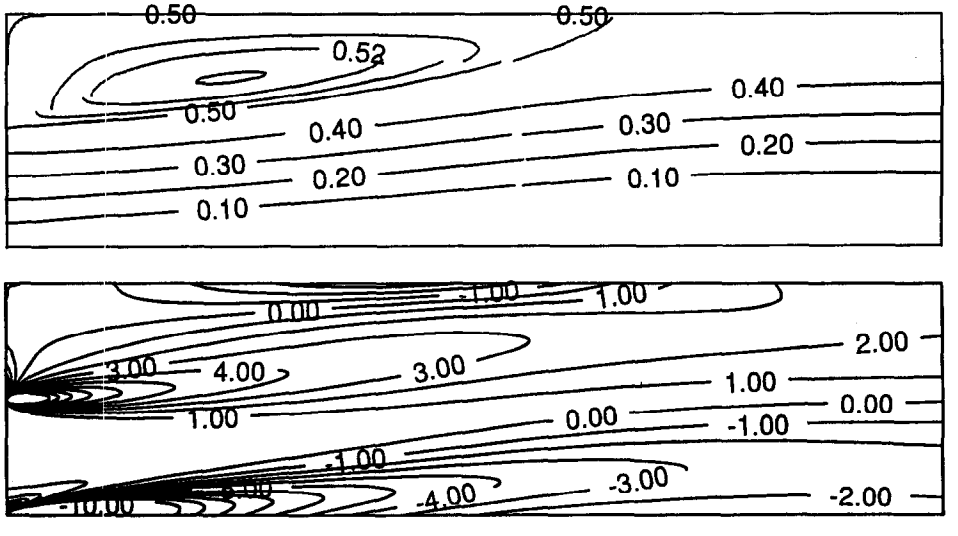

Fig. 9. Streamfunction and vorticity for the sudden expansion at Re = 400.

Tables 6 and 8 allow for comparison of the point and line solvers. A similar pattern emerges for all three discretizations. On coarser grids the line solver has a higher convergence rate, but at the finest level it requires less. This is particularly apparent for the higher order discretizations where the line solver is more suited to their large computational molecules. It should be noted, however, that a full sweep with the line solver takes 100% more CPU time than one full sweep with the point solver, so the point version is still superior. This overhead could be reduced by use of specially written sparse matrix routines as used by [10] who observed an overhead of 50%.

In light of the experience with the lid-driven test case, the point-by-point algorithm was extended to examine the problem of a sudden expansion in a pipe, as this represents a more severe test. In particular, other researchers [12] have experienced difficulties in the application of derivative boundary conditions within a multigrid algorithm. Here the condition imposed at the exit (see Fig. 7) is,

$$\frac{\partial u}{\partial x} = \frac{\partial v}{\partial x} = 0 \tag{16}$$

This condition is applied implicitly within the smoother by setting the coefficient, A_e, to zero whenever the east face of the control volume is on the exit boundary. This condition is applied on all grid levels and no boundary values are transferred between grids as the implicit implementation means that no boundary values are required. Whilst the length of the channel does affect convergence differently for various Reynolds numbers a length:width ratio of 16 was used throughout. Both very high and very low ratios lead to degraded convergence.

The reattachment lengths in Table 9 are in reasonable agreement with those obtained by using the FLOW3D program with a mesh of 20×160 and upwind differencing. These results were obtained using a mesh of 256 points across the pipe and 4096 along it. Contours are shown in Fig. 9. The graph in Fig. 8 shows that multigrid convergence has been achieved and this is further borne out by examining Table 10. Here the convergence rates decrease with finer grids. The rates for Reynolds number 400 are higher. These are thought however to be due to the omission of relaxation of α in the SMART algorithm. Higher Reynolds numbers solutions make more use of non-zero α and require the more sophisticated treatment.

7. CONCLUSIONS

The main conclusion from this work is that it is possible to obtain solutions with high order discretizations on very fine grids by the use of multigrids. The solutions presented here are very accurate and would be impossible to obtain with non-multigrid methods. The use of a high order bounded discretization is seen to present no significant problems to the multigrid technique. Its implementation is further enhanced by defect correction which leads to a more robust solution technique.

The investigation of a line solver reveals that whilst it has the expected benefit of reducing the number of iterations required, this is not sufficient to give an overall saving in computer time. However, such a solver may be useful for solutions at even higher Reynolds numbers or in other flow situations. The solution of a problem with derivative boundary conditions is another extension of the multigrid which was previously seen as problematic, but is now possible and opens the way to further applications.

The main area of future work that is apparent is to extend the ideas to three dimensions. This work is progressing, enhanced by recent developments in computer graphics, and will be reported elsewhere. A further extension to be investigated is application of the algorithms to the modelling of turbulence.

Acknowledgements—The authors wish to acknowledge the continued support of Rolls-Royce plc and the SERC during the course of this work.

REFERENCES

1. P. H. Gaskell, P. A. Sleigh and N. G. Wright, Multigrids and their role in the solution of practical CFD problems. In *Multigrid Methods: Special Topics and Applications II*. Gesellschaft für Mathematik und Datenverarbeitung, Sankt Augustin (1990).

2. P. H. Gaskell and A. K. C. Lau, Curvature compensated convective transport: SMART, a new boundedness preserving transport algorithm. *Int. J. Numer. Meth. Fluids* **8,** 617 (1988).
3. T. M. Shah, Analysis of the Multigrid Method. Ph.D. thesis, Univ. of Oxford (1989).
4. S. V. Patankar and D. B. Spalding, A calculation procedure for heat, mass and momentum transfer in three-dimensional parabolic flows. *Int. J. Heat Mass Transfer* **15,** 1787 (1972).
5. G. Shaw and S. Sivaloganathan, A theoretical and practical smoothing analysis of the SIMPLE pressure-correction algorithm. Technical Report 87/01, Oxford University Computing Laboratory, Numerical Analysis Group (1987).
6. A. Brandt and N. Dinar, Multigrid solution to elliptic flow problems. In *Numerical Methods in Partial Differential Equations* (Edited by S. Parter), pp. 53–147. Academic Press (1977).
7. M. Zedan and G. E. Schneider, Investigation of simultaneous variable solution procedure for velocity and pressure in incompressible fluid flow problems. Technical Report AIAA-83-1519, AIAA (June 1983).
8. P. F. Galpin, J. P. Van Doormaal and G. D. Raithby, Solution of the incompressible mass and momentum equation by application of a coupled equation line solver. *Int. J. Numer. Meth. Fluids* **5,** 615 (1985).
9. S. P. Vanka, Block-implicit multigrid solution of Navier–Stokes equations in primitive variables. *J. Comput. Phys.* **65,** 138 (1986).
10. M. C. Thompson and J. H. Ferziger, An adaptive multigrid technique for the incompressible Navier–Stokes equations. *J. Comput. Phys.* **82,** 94 (1989).
11. C. W. Oosterlee, Robust multigrid methods for the steady and unsteady incompressible Navier–Stokes equations in general coordinates. Ph.D. thesis, Technische Univ. Delft (1993).
12. S. Sivaloganathan. G. J. Shaw, T. M. Shah and D. F. Mayers, A comparison of multigrid methods for the incompressible Navier–Stokes equations. In *Numerical Methods for Fluid Dynamics III* (Edited by Morton and Baines), IMA Conference series, p. 410. Clarendon Press, Oxford (1988).
13. O. R. Burggraf, Analytical and numerical studies of the structure of steady separated flows. *J. Fluid Mech.* **24,** 113 (1966).
14. D. B. Spalding, A novel finite difference formulation for differential expressions involving both first and second derivatives. *Int. J. Numer. Methods Engng* **4,** 551 (1972).
15. P. H. Gaskell and A. K. C. Lau, The method of curvature compensation and its use in the prediction of highly recirculating flows. In *Proceedings of the AIAA/ASME/SIAM/APS 1st National Fluid Dynamics Congress, Part 1,* pp. 272–279 (1988).
16. B. P. Leonard, A stable and accurate convective modelling procedure based on quadratic upstream interpolation. *Comput. Methods Appl. Mech. Engng* **19,** 59 (1979).
17. R. L. Burden, J. D. Faires and A. C. Reynolds, *Numerical Analysis.* Prindle, Weber & Schmidt, Boston (1981).
18. N. G. Wright, Multigrid Solution of Elliptic Fluid Flow Problems. Ph.D. thesis, Univ. of Leeds (1988).
19. P. H. Gaskell and A. K. C. Lau, An efficient solution strategy for use with higher order discretisaton schemes. Technical Report T40, Department of Mechanical Engineering, Univ. of Leeds (1986).
20. U. Ghia, K. N. Ghia and C. T. Shin, High Re solutions for incompressible flow using the Navier–Stokes equations and a multigrid method. *J. Comput. Phys.* **43** (December 1982).
21. W. Hackbusch, *Multi-grid Methods and Applications,* Vol. 4 of Springer Series in Computational Mathematics. Springer (1985).
22. S. Sivaloganathan and G. Shaw, A multigrid method for recirculating flows. *Int. J. Numer. Methods Fluids* **8,** 441 (1988).
23. S. A. E. G. Falle and M. J. Wilson, Multigrid calculation of jet flows. In *Numerical Methods for Fluids Dynamics III* (Edited by Morton and Baines), IMA Conference Series, p. 418. Clarendon Press, Oxford (1988).
24. C. W. Oosterlee and P. Wesseling, A multigrid method for an invariant formulation of the incompressible Navier–Stokes equations in general coordinates. Technical Report 91-12, Faculty of Mathematics and Informatics, Delft University of Technology (1991).
25. W. Hackbusch, *Robust Multigrid Methods,* Vol. 23 of Notes on Numerical Fluid Dynamics. Vieweg (1988).
26. A. K. C. Lau, Mathematical Modelling of Non-Reacting Recirculation Flows. Ph.D. thesis, Univ. of Leeds (1987).
27. J. Linden, G. Lonsdale, B. Steckel and K. Stüben, Multigrid for the steady-state incompressible Navier-Stokes equations: a survey. Technical Report 322, Gesellschaft für Mathematik und Datenverarbeitung (1988).
28. A. Brandt and I. Yavneh, Inadequacy of first-order upwind difference schemes for some recirculating flows. *J. Comput. Phys.* **93,** 128 (1991).